Hyperbaric Oxygen Therapy for Veterans With Combat-Associated Posttraumatic Stress Disorder:

A Randomized, Sham-Controlled Clinical Trial

Keren Doenyas-Barak, MD; Ilan Kutz, MD; Erez Lang, MD; Amir Assouline, PhD; Amir Hadanny, MD, PhD; Kristoffer C. Aberg, PhD; Gabriela Levi, MA; Ilia Beberashvili, MD; Avi Mayo, PhD; and Shai Efrati, MD

Abstract

Objective: Cumulative data indicate that new protocols of hyperbaric oxygen therapy (HBOT) may induce neuroplasticity and improve clinical symptoms of patients suffering from posttraumatic stress disorder (PTSD). The aim of the current study was to evaluate the effects of HBOT on veterans with combat-associated PTSD (CA-PTSD) in a randomized, sham-controlled trial.

Methods: Male veterans aged 25–60 years with CA-PTSD, with a Clinician-Administered PTSD Scale for *DSM-5* (CAPS-5) score above 20, were included. Exclusion criteria included a history of traumatic brain injury, other psychiatric diseases, or contraindication to HBOT. Participants were randomly assigned to HBOT or sham intervention. Both interventions involved 60 daily sessions, with 90 minutes of either 100% oxygen at 2 atmospheres absolute (ATA) (HBOT) or 21% oxygen at 1.02 ATA (sham) with 5-minute air breaks every 20 minutes. CAPS-5 score, Beck Depression Inventory-II (BDI-II), the Depression, Anxiety and Stress Scale 21 Items (DASS-21), and resting-state functional magnetic resonance imaging (rsfMRI) were assessed at baseline and posttreatment, with the primary end point defined as a 30% reduction in CAPS-5 score from baseline.

Results: The study was conducted between February 2020 and July 2023. Of 63 veterans who underwent randomization, 56 completed the study protocol (28 in each group). The HBOT group showed a significant decrease in mean CAPS-5 total score, from 42.57 ± 9.29 at baseline to 25.8 ± 9.5 following HBOT ($P < .001$) and 25.08 ± 13.08 at follow-up ($P < .001$). The sham group demonstrated a significant increase in CAPS-5 total score from baseline to follow-up, from 45.11 ± 8.99 to 47.75 ± 11.27 following HBOT ($P = .069$) and 49.22 ± 10.26 at follow-up ($P = .011$). Significant improvements in the depression domain of the DASS-21 questionnaire and BDI-II were demonstrated ($F = 4.55$, $P = .03$ and $F = 4.2$, $P = .04$, respectively). The stress and anxiety domains of DASS-21 did not reach statistically significant levels. Analysis of rsfMRI demonstrated improved connectivity within the 3 main networks (default-mode network, central-executive network, salience network) in HBOT vs sham groups.

Conclusions: Dedicated HBOT protocol can improve PTSD symptoms of veterans with CA-PTSD. The clinical improvement was accompanied by enhanced functional connectivity demonstrated by rsMRI.

Trial Registration: ClinicalTrials.gov identifier: NCT04518007

J Clin Psychiatry 2024;85(4):24m15464

Author affiliations are listed at the end of this article.

Posttraumatic stress disorder (PTSD) leads to lasting social, behavioral, and occupational dysfunctions and affects a substantial proportion of veteran combatants.[1] Despite advancements in both psychological and pharmacologic treatments, many individuals with PTSD do not experience remission.[2] Additionally, treatment nonresponse rates are high, particularly in the military and veteran populations, with two-thirds of the treated population retaining a PTSD diagnosis after receiving treatment.[3] Real-world data on treatment effectiveness, based on the Israeli Ministry of Defense clinics, show a remission rate of 39.4%, with remission rates for intrusive symptoms being lower than 15%.[2] Modest treatment response rates were also demonstrated among veterans with military-related PTSD in the United States and Australia.[4,5] Emerging research suggests that persistent PTSD symptoms may be rooted in biological changes in brain activity and structure.[6–9] Functional magnetic resonance imaging (fMRI) studies reveal disruptions in the frontolimbic

Clinical Points

- While data suggest hyperbaric oxygen therapy (HBOT) benefits for veterans with posttraumatic stress disorder (PTSD), there is a significant lack of sham-controlled trials focused solely on military-related PTSD without traumatic brain injury. This study addresses that gap.
- HBOT targets the biological impacts of trauma and should be considered for veterans with PTSD who are unresponsive to psychotherapy and pharmacotherapy.
- HBOT should be administered only in medical-standard facilities with staff trained in PTSD-specific challenges.

circuit, indicating impaired control of the prefrontal cortex over the limbic system among PTSD patients when compared to non-traumatized or traumatized healthy individuals.[6–9] Insights regarding the role of brain activity changes in the non-remitting nature of PTSD have prompted scientists and clinicians to pursue biological interventions that can facilitate neuroplasticity. One of the measured objective outcomes of neuroplasticity includes changes in brain network connectivity as evaluated using resting-state fMRI (rsfMRI).[10] In recent years, a growing body of evidence has emerged regarding the neuroplasticity-inducing effects of new hyperbaric oxygen therapy (HBOT or HBO2) protocols.[11–14] We know today that the fluctuations between hyperoxia and normoxia on the cellular level, induced by HBOT, stimulate stem cell activity, promoting their migration and differentiation, trigger mitochondrial proliferation and biogenesis, facilitate mitochondrial transfer, and foster angiogenesis.[11] This phenomenon, termed the "hyperoxic-hypoxic paradox," was shown both clinically and via imaging to contribute to improvements even years after acute insults, across various conditions including chronic poststroke, postconcussion, and post-COVID patients.[13,15–17] The beneficial effects of HBOT on combat-associated PTSD (CA-PTSD) were previously demonstrated in an open-label controlled trial involving a similar cohort of veterans with PTSD.[18] A long-term follow-up study, conducted 704 ± 230 days postcompletion of the HBOT course, revealed persisting treatment results.[19] Additionally, 10 previous studies[12,20–27] including 6 controlled trials[14,22,25–28] evaluated the effect of HBOT on PTSD. In 4 of them, patients were recruited for traumatic brain injury (TBI), but the impact of HBOT on posttraumatic symptoms was evaluated as well.[22,25–27] HBOT has a positive effect on postconcussion symptoms, and due to the potential overlap between posttraumatic and postconcussion symptoms, differentiating the effects of the treatment on each of these diagnoses might be difficult. Thus, the current study aims to evaluate the efficacy and safety of HBOT on veterans with CA-PTSD, without a known previous TBI.

MATERIALS AND METHODS

Study Design and Patients

The study was a randomized, sham-controlled trial conducted at the Sagol Center for Hyperbaric Medicine and Research at the Shamir Medical Center, Israel, between February 2020 and July 2023. The protocol was approved by Shamir's Institutional Review Board (291/19) and was registered with ClinicalTrials.gov (NCT04518007).

Patients were referred to the study by their psychiatrist or psychotherapist, or by expressing interest after learning about the treatment from fellow veterans. The study included male veterans, aged 25–60 years, with CA-PTSD lasting 5 or more years prior to their inclusion. Patients were recruited if they had persistent residual debilitating PTSD symptoms after being treated with at least 1 course of trauma-focused psychotherapy and pharmacotherapy, and still fulfilled the Clinician-Administered PTSD Scale for *DSM-5* (CAPS-5) diagnostic criteria for PTSD with a score over 20. Exclusion criteria included a history of TBI or any other known brain pathology; active malignancy; substance or alcohol misuse at baseline (except for prescribed cannabis, in either nebulized or tincture forms); active manic or psychotic episodes; serious current suicidal ideation; severe or unstable physical disorders or major cognitive deficits at baseline; previous HBOT treatments; chest, ear, or sinus pathologies incompatible with pressure changes; inability to perform an awake brain MRI; active smoking; and inability to read and sign an informed consent form.

Randomization and Masking

Eligible candidates were randomized with equal probability to the HBOT and sham interventions. After randomization, when a cluster of 4–6 subjects from one of the arms was filled, the intervention for that cluster was initiated within the HBOT/sham chamber, which accommodates up to 6 subjects.

Patients, physicians, therapists, and assessors were blinded to the intervention assignment. The randomization code was generated by a coordinator who was masked to the study and was not involved in the study's execution. To evaluate the blinding, following the first HBOT/sham session, patients were asked to discreetly answer a questionnaire about their perception of whether they were allocated to the treatment or sham group. All data were stored in a dedicated database and were checked for accuracy and completeness.

Procedures

After signing an informed consent form, patients underwent a baseline evaluation, including a medical history review, a physical examination, a clinical

interview by 2 senior clinicians, psychiatric evaluation by a psychiatrist, filling of questionnaires, and a brain MRI.

Both the HBOT and sham protocols were conducted in a multiplace Starmed-2700 chamber (HAUX-Life-Support GmbH, Germany). The protocol comprised 60 daily sessions, 5 days per week. Protocol completion was limited to 14 weeks in case of missed sessions. Due to the COVID-19 isolation regimens, extension of the treatment period was allowed in specific cases.

HBOT protocol. Each HBOT session consisted of 90 minutes' exposure to 100% oxygen at 2 atmospheres absolute (ATA) with 5-minute air breaks every 20 minutes.

Sham protocol. Each sham session consisted of 90 minutes' exposure to 21% oxygen by mask at 1.02 ATA for 90 minutes. To achieve blinding and have the subjects perform pressure equalization, compression to 1.2 ATA was performed for the first 5 minutes, followed by slow decompression to 1.02 ATA in the following 5 minutes. The minimal added 0.02 ATA was required to maintain the chamber door shut.

Meetings of the study participants with study investigators were scheduled every 2 weeks during the HBOT/sham period to monitor symptoms and evaluate potential adverse events.

Patients in both groups continued their psychological and pharmacologic treatments as they did before their inclusion, acknowledging that some may not have had active treatment at inclusion. Any changes in the frequency of psychological treatments or pharmacotherapy doses were reported and documented.

Outcomes

The primary end points were responder rates, defined as a 30% reduction of CAPS score from baseline.[29]

Secondary end points included changes in PTSD symptoms load, based on CAPS-5 scores and remission rates, defined as CAPS scores lower than 20, severity of depression evaluated by the Beck Depression Inventory-II (BDI-II) and severity of anxiety, somatization, and stress as evaluated by the Depression, Anxiety and Stress Scale 21-Item (DASS-21) questionnaire. The interview and inventories were administered by the study investigators at baseline, after 1–4 weeks, and 3 months after the last HBOT/sham session. Brain connectivity was evaluated using the rsfMRI sequence during brain MRI imaging performed at baseline and after 1–4 weeks from the last HBOT or sham session.

CAPS-5. CAPS-5 is a structured interview–based test that consists of 30 items. Items are rated on a 0 to 4 severity scale. Twenty of the items are summed to give a score that reflects the severity of *DSM-V* PTSD symptoms and served as the primary end point. The score ranges between 0 and 80, with higher scores indicating more severe PTSD symptoms.[30]

BDI-II. BDI-II is a widely used psychometric test for measuring the severity of depression. It consists of 21 multiple-choice questions and a self-report inventory about how the subject has been feeling in the last week. Each answer is scored on a scale of 0–3. The score ranges between 0 and 63, with higher scores indicating more severe depression symptoms.[31]

DASS-21. DASS-21 is a 3-part self-report scale designed to measure the emotional state of depression, anxiety, and stress. Each of the 3 scales contains 7 items, divided into subscales with similar content. The summed numbers in each subscale are then multiplied by 2 to obtain total scores that can be compared to the original DASS-42. Scores range between 0 and 42 in each subcategory, with higher scores reflecting severity.[32]

Brain imaging data acquisition. MRI scans were performed on a MAGNETOM Vida 3T Scanner, configured with a 64-channel receiver head coil (Siemens Healthcare, Erlangen, Germany). The MRI protocol included 3D T2-weighted, 3D fluid attenuated inversion recovery, susceptibility weighted imaging, high-resolution T1-weighted (magnetization-prepared rapid acquisition with gradient echo), and blood oxygen level dependent (BOLD).

The BOLD sequence consisted of 300 volume measurements of gradient-echo (echo-planar imaging) contrast sequences. Scan parameters are as follows: repetition time: 1,500 milliseconds, echo time: 30 milliseconds, flip angle: 90°, voxel size: 2.2 × 2.2 × 3.0 mm, distance factor: 25%, field of view: 210, number of slices: 36, axial slices parallel to the AP-PC plane. During the scanning process, each participant was instructed to remain motionless and relaxed, with their eyes open, and to refrain from engaging in deliberate thoughts. Foam pads and earplugs were utilized to minimize head movement and scanning noise.

BOLD preprocessing. Functional connectivity was analyzed using the CONN-fMRI Toolbox v17 (https://www.nitrc.org/projects/conn) and SPM v12 (https://www.fil.ion.ucl.ac.uk/spm/software/spm12/). A flexible preprocessing pipeline was conducted including realignment with correction of susceptibility distortion interactions, slice timing correction, outlier detection, direct segmentation, and Montreal Neurological Institute-space normalization and smoothing (see full description in Supplementary Materials).

Sample size. The sample size of the study was calculated using G*Power software, version 3.1.9.7. The sample size calculation was based on the results of a previous study in a similar cohort with HBOT.[18] According to that study, 71% of patients in the HBOT group responded to HBOT. The expected response in the sham group was 32%.[33] Using the *z*-test method, a sample size of 28 patients in each group allows for an 85% statistical power, with a 2-sided significance of .05, to detect a 39% difference in treatment response between the intervention and placebo groups. Considering the dropout rate of 15% according to a previous study,[18] the sample size was determined to be

Figure 1.
Study Flowchart

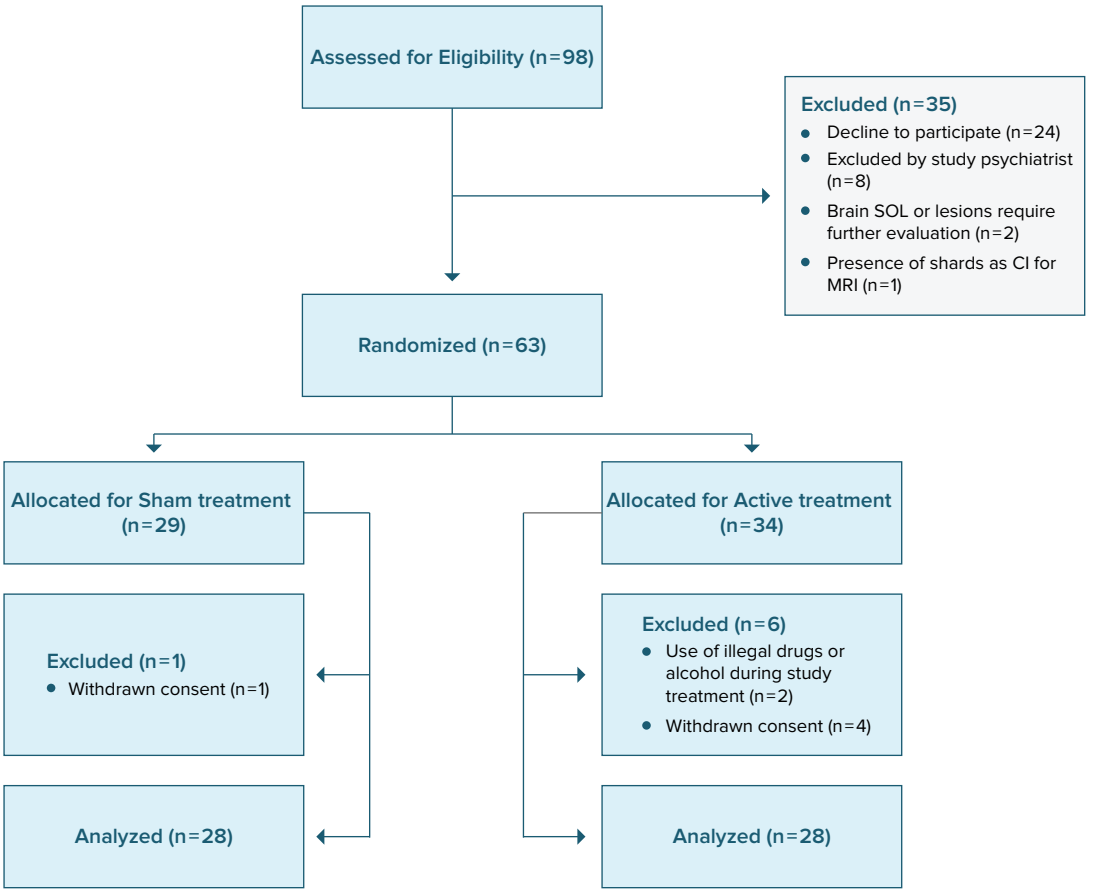

Abbreviations: CI = contraindication, MRI = magnetic resonance imaging, SOL = Space Occupying Lesion

70 patients. However, due to a higher-than-expected dropout rate, the sample size was increased following approval to 98. The study was analyzed as intention-to-treat, meaning that patients were included in the analysis if they attended at least 1 session of HBOT/sham and completed the assessments.

Data analysis. Continuous data were expressed as means ± standard deviations, or as medians and interquartile ranges (quartiles 1–3) if variables did not follow a normal distribution. Categorical variables were expressed as frequencies. Normally distributed variables were compared between the 2 groups using a *t* test (2-sided). Nonparametric *U* tests (Mann-Whitney) were performed to compare variables with skewed distributions, and categorical data were compared between the 2 groups with χ^2 tests. The differences between the 2 groups at the 3 different timepoints, as well as the effect of the intervention (HBOT vs sham) on changes in the study variables (interaction effect between time and group), were analyzed using mixed repeated-measures analysis of variance (ANOVA). Data were analyzed using SPSS software (version 28.0).

rsfMRI data analysis. Individual connectivity maps were generated utilizing the seed-to-voxel approach. We focused on a priori seeds obtained from the CONN-fMRI Toolbox, Harvard Oxford Atlas, specifically targeting commonly reported large-scale brain networks associated with PTSD. These networks include the default mode, salience, frontoparietal (also known as the central executive network), hippocampus, amygdala, and thalamus.[34] Bivariate correlation analysis was used to determine the linear association between the seed and significant voxel clusters. On the group level, a mixed repeated-measures ANOVA model was utilized to assess the primary interaction effect between time and group. *P* values were adjusted for multiple correlations using the false discovery rate procedure ($P < .05$).

RESULTS

Ninety-eight patients signed the informed consent form. Thirty-five were excluded before randomization:

Table 1.
Baseline Characteristics[a]

	HBOT	Sham
N	28	28
Age, y	37.75 ± 8.29	36.4 ± 7.36
Marital status		
Single	9 (32.1)	13 (46.4)
Married	15 (53.6)	15 (53.6)
Divorced	4 (14.3)	0
No. of children	3.05 ± 2.0	2.6 ± 1.3
Education, y	13.86 ± 2.89	14.0 ± 3.4
Working	17 (60.7)	13 (46.4)
Service duration	7.84 ± 8.3	7.2 ± 2.6
Time from last combat exposure	12.4 ± 7.62	12.0 ± 6.8
Mild (CAPS 20–39)	10 (35.7)	8 (28.57)
Moderate (CAPS 40–59)	17 (60.71)	19 (67.9)
Severe (CAPS 60–80)	1 (3.6)	1 (3.6)
Total CAPS score	42.57 ± 9.28	45.11 ± 8.98
Current major depression	15 (53.6)	17 (60.7)
Medications		
SSRIs/SNRIs	10 (28.5)	11 (42.86)
Antipsychotic	6 (14.25)	5 (17.86)
Benzodiazepines	3 (10.71)	5 (17.86)
Cannabis	11 (32.14)	14 (46.43)
Cannabis (g per month)	28.64 ± 12.27	37.86 ± 13.69
Baseline questionnaires		
BDI-II	28.67 ± 10.26	32.32 ± 10.86
Depression (DASS-21)	11 ± 4.40	11.36 ± 4.57
Anxiety (DASS-21)	10.14 ± 5.19	9.68 ± 5.39
Stress (DASS-21)	14.29 ± 4.73	15.32 ± 4.71

[a]Continuous variables are expressed as mean ± standard deviation. Categorical variables are expressed as number (percentage). Normally distributed continuous variables were compared by *t* test, nonnormal continuous variables were compared between the groups by the Mann-Whitney *U* test, and χ^2 tests were used to compare categorical variables.

Abbreviations: BDI-II = Beck Depression Inventory-II, CAPS-5 = Clinician-Administered PTSD Scale for *DSM-5*, DASS-21 = Depression Anxiety Stress Scale-21, HBOT = hyperbaric oxygen therapy, SNRI = serotonin-norepinephrine reuptake inhibitor, SSRI = selective serotonin reuptake inhibitor.

24 could not commit to the study schedule, 8 were excluded by the study psychiatrist due to psychiatric exclusion criteria conditions, 2 were excluded due to brain pathologies diagnosed on baseline MRI, and 1 subject was excluded due to the presence of shrapnel that precluded the performance of MRI. Of the remaining 63 patients, 6 were excluded, 2 were excluded due to the use of illegal drugs and alcohol during the study treatment course, and 4 withdrew consent (Figure 1). Accordingly, 28 patients from the HBOT group and 28 patients from the sham group who completed at least 1 session and the study assessments were included in the clinical analysis. All participants except 8 patients in the sham group completed at least 50 sessions; the mean number of sessions completed by the HBOT group was 59.92 (58–60) and by the sham group was 52.42 (20–60). Baseline characteristics are summarized in Table 1. There was no significant difference between the groups in any of the baseline characteristics.

Blinding Evaluation

Patient blinding was found to be reliable, where the treatment perception rate did not differ between the 2 groups. In both the HBOT and sham groups, 64% of the participants assumed they were receiving HBOT while 36% assumed they were receiving sham treatment ($P = 1.0$; Supplementary Figure 1).

Primary Outcome

Treatment response rates were 68% vs 4% at the end of HBOT/sham treatment ($P < .001$) and 61% vs 4% at the end of follow-up, respectively ($P < .001$).

The results of the CAPS score are summarized in Table 2. A significant improvement in all CAPS symptom clusters was demonstrated in the HBOT arm, while no improvement was seen in the sham group. A significant group-by-time interaction ($F = 27.33$, $P < .001$) was demonstrated between the groups (Table 2; Figure 2). Seven patients (25%) achieved remission in the HBOT group compared to 1 (3.6%) in the sham group by the end of the treatment ($P < .01$). Additionally, at follow-up, 11 patients (39.2%) in the HBOT group achieved remission, whereas none did in the sham group ($P < .01$).

Secondary End Points

BDI and DASS-21 questionnaire analyses are summarized in Table 2. On the BDI, there was a significant improvement in the HBOT group as compared to the sham group ($F = 4.2$ and $P = .043$). Significant improvements in the depression domain of the DASS-21 questionnaire were also demonstrated in the HBOT group as compared to the sham group ($F = 4.55$, $P = .034$). The stress and anxiety domains of DASS-21 did not reach statistically significant levels.

rsfMRI Analysis

Of the 56 included patients, 1 patient did not complete the full 7.5-minute rsfMRI sequence, and 2 patients were omitted due to inconsistencies in scanning parameters, leaving 25 in the sham group and 28 in the HBOT group.

Seed-to-voxel functional connectivity analysis revealed significant group-by-time interactions in connectivity patterns across diverse brain networks in the HBOT group compared to the sham group. Specifically, there was a notable increase in functional connectivity between the left and right thalami, acting as seeds, and pivotal nodes within the frontoparietal network, including the left and right posterior parietal cortex, the left and right lateral prefrontal cortex, and the angular and supramarginal gyri (Figure 3; Supplementary Table 1).

An augmentation in functional connectivity was evident within the default mode network, particularly between the medial prefrontal cortex as a seed and the lingual gyrus (Figure 3; Supplementary Table 1).

Table 2.
Questionnaire Results[a]

	HBOT				Control				Effect size (Cohen *d*) post-HBOT	Effect size (Cohen *d*) follow-up	Group-by-time interaction (*F*)[d]	*P* value[d]
	Baseline	Post-HBOT	*P* value[b]	Follow-up	*P* value[c]	Baseline	Post-HBOT	*P* value[b]	Follow up	*P* value[c]				
CAPS score[e]														
B	11.43 ± 3.05	6.93 ± 4.0	<.001	6.82 ± 4.16	<.001	11.86 ± 3.06	12.71 ± 3.67	.088	12.81 ± 3.66	.1	1.83	1.83	15.89	<.001
C	5.18 ± 1.49	2.89 ± 2.0	<.001	2.36 ± 1.9	<.001	5.46 ± 1.58	5.46 ± 1.91	1	5.59 ± 1.67	.68	1.43	1.91	18.91	<.001
D	13.5 ± 4.38	8.07 ± 3.55	<.001	7.79 ± 5.16	<.001	15.36 ± 3.90	15.57 ± 4.97	.79	16.22 ± 4.7	.36	1.3	1.27	14.57	<.001
E	12.46 ± 3.27	7.93 ± 2.87	<.001	8.32 ± 3.58	<.001	12.43 ± 3.28	14.00 ± 3.94	.05	14.59 ± 2.95	.01	2.46	2.21	23.59	<.001
Total	42.57 ± 9.29	25.82 ± 9.5	<.001	25.08 ± 13.08	<.001	45.11 ± 8.99	47.75 ± 11.27	.069	49.22 ± 10.26	.011	2.64	2.28	27.33	<.001
BDI	28.67 ± 10.26	19.03 ± 13.62	<.001	19.27 ± 14.54	<.001	32.32 ± 10.86	27.39 ± 13.71	.02	30.62 ± 14.24	.22	0.41	0.53	4.2	.043
DASS-21														
Depression	22 ± 8.8	17.88 ± 10.88	.011	15.62 ± 12.67	.008	22.7 ± 9.14	23.64 ± 10.37	.31	24.83 ± 9.6	.26	0.53	0.54	4.55	.034
Anxiety	20.28 ± 10.38	18.08 ± 11.68	.133	7.23 ± 6.72	.016	19.36 ± 10.8	20.42 ± 12.00	.26	20.42 ± 10.28	.27	0.35	0.26	2.76	.098
Stress	28.58 ± 9.14	23.15.6 ± 11.54	.012	22.08 ± 11.98	<.001	30.64 ± 9.42	30.14 ± 9.97	.386	30.33 ± 9.6	.47	0.44	0.4	2.34	.128

[a]Data are presented as mean ± SD.
[b]Pre-post treatment/sham *P* value.
[c]Pre-follow-up posttreatment/sham *P* value.
[d]*F* and *P* values for group-by-time interaction, using a linear mixed model.
[e]B = criterion B, reexperiencing symptoms; C = criterion C, avoidance symptoms; D = criterion D, negative alterations in cognitions and mood; E = criterion E, arousal and reactivity symptoms.
Abbreviations: BDI-II = Beck Depression Inventory-II, CAPS-5 = Clinician-Administered PTSD Scale for *DSM-5*, DASS-21 = Depression Anxiety Stress Scale-21, HBOT = hyperbaric oxygen therapy.

Elevated functional connectivity was also observed in frontoparietal network hubs, showcasing heightened connectivity between the left lateral prefrontal cortex and the bilateral thalami, and between the right lateral prefrontal cortex and the supramarginal and angular gyri, the putamen, insula, precuneus, and right frontal pole (Figure 3; Supplementary Table 1).

Within the salience network, increased connectivity was noted between the bilateral rostral prefrontal cortex and the right frontal pole (Figure 3; Supplementary Table 1). There were no significant group-by-time connectivity decreases in all seeds.

The hippocampi and amygdala as seeds had no significant group-by-time interactions based on seed-to-voxel analysis.

Safety and Side Effects

HBOT and sham treatments were both well tolerated, with 23 documented mild and self-limited adverse events in the HBOT group and 15 mild and self-limited events in the sham arm (Table 3). A total of 8 events of self-remitting barotrauma, defined as reported ear pain accompanied by tympanic membrane redness or hematoma, were documented, 6 in the HBOT group and 2 in the sham group. Seven subjects from the HBOT group reported surfacing of new memories during the HBOT course. This phenomenon was accompanied by distress that made the patients report memory surfacing and seek professional advice. The patients were reassured that, based on previous study in similar populations,[35] this is an expected phenomenon. The distress persisted for several days and was followed by resolution. None of the sham group patients reported surfacing of new memories.

DISCUSSION

The current study evaluates, for the first time in a sham-controlled study, the effect of HBOT on veterans suffering from CA-PTSD without previous TBI. HBOT induced significant reductions in PTSD symptom severity, as evaluated by CAPS-5 scores, and reductions in depression symptoms, as evaluated by the BDI-II and DASS-21 questionnaires. In accordance with the clinical improvement, brain connectivity, evaluated by rsfMRI, significantly increased in the frontoparietal network, the default mode network, and the connectivity between the right dorsolateral prefrontal cortex and the thalamus.

Previous controlled studies have shown the positive effect of HBOT on posttraumatic symptoms.[14,22,25–28] Two of the studies that used lower doses of hyperbaric therapy as control treatment showed improvement of posttraumatic symptoms in the so-called sham arm.[26,27] It is well known today that HBOT provided at low pressure can induce significant biological effects[36,37] and

Figure 2.
CAPS Score at Baseline (Base) After HBOT/Sham and at Follow-Up (FU)[a]

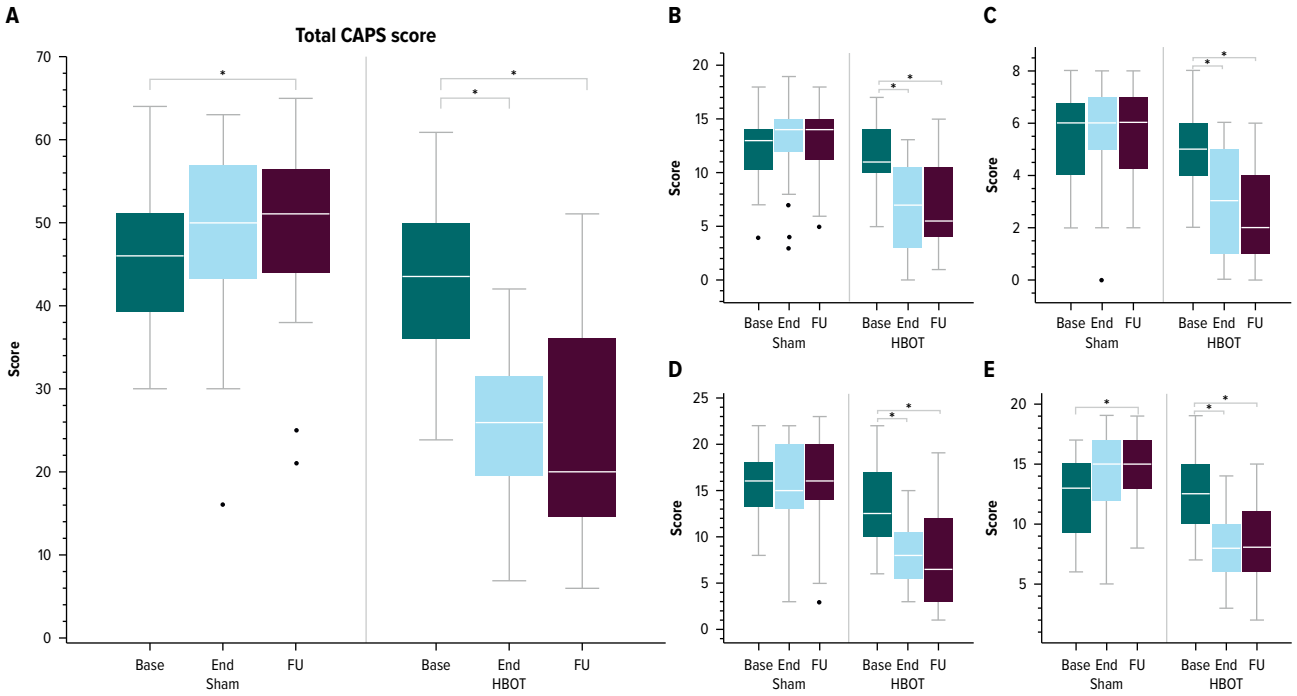

[a]B = criterion B, reexperiencing symptoms; C = criterion C, avoidance symptoms; D = criterion D, negative alterations in cognitions and mood; E = criterion E, arousal and reactivity symptoms. *$P < .05$.
Abbreviations: CAPS-5 = Clinician-Administered PTSD Scale for *DSM-5*, HBOT = hyperbaric oxygen therapy.

thus should not be regarded as sham.[36,37] In the current study, we used a dedicated sham protocol previously shown to have masking and no significant biological effect.[17,38] As in previous studies using the same sham protocol, patient blinding was found to be reliable.[39–41] Along with the biological effects observed in previous HBOT studies, their shorter treatment duration and the short-term evaluation might have contributed to additional significant placebo effects.

The current study comprised 60 daily sessions over a three-month period, and thus, any temporary improvements often seen with sham treatments due to the participation effect[42] should vanish over this time period. Therefore, making the effort to attend 60 daily sessions poses a significant time and resource demand on these patients. The lack of clinical improvement potentially discouraged patients in the sham group, as reflected by 8 patients who ended the HBOT sessions earlier. Lastly, the characteristics of the current study's population who suffered from long-standing PTSD and failed to have a significant beneficial response to previous treatments might also contribute to lower placebo effects in the sham treatment than usually reported.[33]

In the past decade, cross-sectional studies have revealed rsfMRI alterations in individuals with PTSD. rsfMRI is being used to measure the correlation between brain activation patterns across different regions, reflecting the synchronization of neural activity during periods of rest. Notably, it has been proposed that changes in specific networks, the default mode network, the frontoparietal network, and the salience network, may underlie PTSD symptoms.[43] The thalamus has also garnered recent attention in the context of PTSD.[34]

The default mode network, which encompasses the medial prefrontal cortex, posterior cingulate cortex, precuneus, and temporoparietal regions, is implicated in self-referential processing, with decreased connectivity associated with PTSD symptoms.[43] In the current study, there was a significant increase in functional connectivity between the medial prefrontal cortex and high-level visual areas following HBOT.

The salient network, which includes the dorsal anterior cingulate cortex, rostral prefrontal cortex, and insula, is associated with attentional processes.[43] We found the rostral prefrontal cortex exhibits enhanced connectivity with the right frontal pole following HBOT.

The frontoparietal network includes centers around the dorsolateral prefrontal cortex and is involved in higher-order executive functioning and emotion regulation with significant relevance to PTSD functional connectivity patterns.[44] Our analysis found amplified connectivity in the HBOT group, between the

Figure 3.
Significant Seed-to-Voxel Functional Connectivity Group-by-Time Interactions[a],*

A. Left and right thalamus[a]

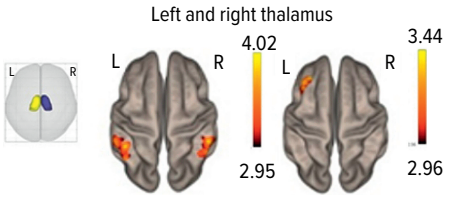

B. Default-mode network[b]

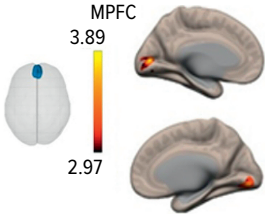

C. Frontoparietal network[c]

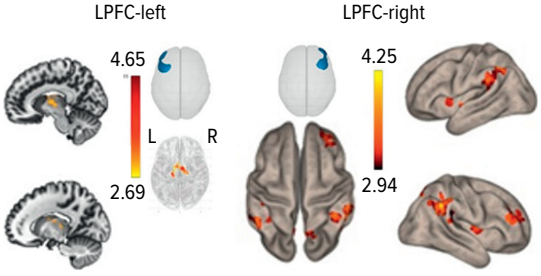

D. Salience network[d]

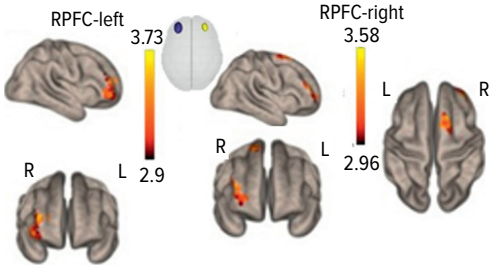

[a]The seed regions include both thalami. The clusters that were highly correlated with the bilateral thalami include the inferior parietal lobule (left and right) and the midfusiform gyrus.
[b]The seed region is the medial prefrontal cortex. The clusters with high correlation with the medial prefrontal cortex include regions in the lingual gyrus and calcarine cortex.
[c]The seeds are left and right prefrontal cortex. The left prefrontal cortex shows high correlation with the bilateral thalami. The right PFC is highly correlated with the supramarginal and angular gyrus.
[d]The seeds are the left and right RPFC. Both seeds show high correlation with the right frontal pole. Additionally, the right RPFC is also highly correlated with the superior frontal gyrus.
*Voxel significance was set at $P < .005$; cluster significance was set at $P < .05$, with false discovery rate correction applied. The colored patches on the brain images and the bars (representing *T* test statistics) indicate significantly higher posttreatment connectivity compared to pretreatment in the treatment group (+1) vs the sham group (–1).
Abbreviations: LPFC = lateral prefrontal cortex, MPFC = medial prefrontal cortex, PFC = prefrontal cortex, RPFC = rostral prefrontal cortex.

Table 3.
Adverse Events

	HBOT	Sham
Barotrauma[a]	6	2
Recovery of new memories[a]	7	0
Viral infection	4	4
Cannabis overdose	1	0
Abnormal laboratory test[b]	1	2
Epistaxis	0	1
Headache and musculoskeletal pain	0	3
Trauma (head, eye, ankle)	2	1
Extravasation of contrast media	0	1
Dyspnea	1	0
Tenesmus	1	0
Temporal confusion	0	1
Total	**23**	**15**

[a]Statistically significant difference between the groups with $P < .05$.
[b]Elevated thyroid-stimulating hormone, elevated liver function tests, and elevated creatine kinase.
Abbreviation: HBOT = hyperbaric oxygen therapy.

dorsolateral prefrontal cortex and the inferior parietal areas including the supramarginal gyrus and the angular gyrus, the precuneus, and the thalamus.

Decreased connectivity of the thalamus has been shown to characterize PTSD patients.[45] We demonstrated increased connectivity of the left thalamus with the right inferior parietal lobe, bilateral supramarginal and right angular gyri, and the right thalamus with the left middle frontal gyrus.

We did not find any decrease in functional connectivity following the treatment within the HBOT group compared to the sham group. The consistency of these results across studies further substantiates the neural basis for the clinical improvements observed following HBOT.

The current study has several limitations. A 28-patient cohort in each group may be considered small. However, the sample size did not compromise the significance of the results. Additionally, the relatively short-term follow-up of 3 months in the current study may not fully reflect changes in the disorder's course. However, it is worth noting that a previous study,[18] which evaluated long-term effects 2 years after treatment cessation, suggests long-lasting effects of HBOT, contributing to the expected long-term effects in the

current study. Another limitation may be related to the study generalizability. Given the rigorous nature of the trial and the significant demands on participants, it is possible that the study population may predominantly consist of individuals experiencing a substantial symptom burden.

In 2018, the Veterans Affairs (VA) evidence-based synthesis program for TBI and PTSD stated that, based on the data available up to 2018, it was difficult to make clear decisions regarding the use of HBOT for PTSD[46] and that further research in this field is needed. In 2023, the VA/Department of Defense Clinical Practice Guideline for PTSD stated that the available studies suggested a benefit for HBOT on the outcome of PTSD; however, the absence of an adequate control condition limits the confidence in these results. The present data, together with previous studies in the same population,[18,19] fill this gap and may thus support the recommendation of future guidelines for providing HBOT to many veterans with PTSD who are refractory to first-line recommended treatments.

When applying the study's results for the treatment of posttraumatic veterans, it is extremely important to adhere to the evidence-based, proven protocol detailed in the current study. The currently used protocol that includes 60 daily sessions, 5 days per week, with 2 ATA, 100% oxygen, and 5-minute air breaks every 20 minutes has been shown to induce neuroplasticity and recovery of posttraumatic symptoms.[47] The study's conclusions should not be used to encourage hyperbaric treatments in non–medical grade facilities, variations of monoplaces, home used chambers, or clinics without a professional multidiscipline medical team. Furthermore, given the potential for symptom worsening and memory surfacing during the treatment course, patients should be committed to the full course of at least 60 sessions, and the treatment protocol should be provided only by centers with professionals in the field of PTSD treatment to avoid patient risk.

CONCLUSION

HBOT presents a novel therapeutic approach for PTSD, targeting the biological consequences of traumatic events. This randomized sham-controlled trial demonstrates that HBOT can improve brain connectivity and alleviate PTSD-related symptoms in veterans with CA-PTSD. Taken together, the treatment's safety profile and efficacy support its use for veterans not responding to psychotherapy.

Article Information

Published Online: November 10, 2024. https://doi.org/10.4088/JCP.24m15464

Submitted: June 13, 2024; accepted August 26, 2024.

To Cite: Doenyas-Barak K, Kutz I, Lang E, et al. Hyperbaric oxygen therapy for veterans with combat-associated posttraumatic stress disorder: a randomized, sham-controlled clinical trial. *J Clin Psychiatry*. 2024;85(4):24m15464.

Author Affiliations: Sagol Center for Hyperbaric Medicine and Research, Shamir Medical Center, Zerifin, Israel (Doenyas-Barak, Kutz, Lang, Assouline, Hadanny, Levi, Efrati); Tel Aviv School of Medicine, Tel Aviv University, Tel Aviv, Israel (Doenyas-Barak, Lang, Hadanny, Beberashvili, Efrati); Nephrology Department, Shamir Medical Center, Zerifin, Israel (Beberashvili); Department of Brain Sciences, Weizmann Institute of Science, Rehovot, Israel (Aberg, Beberashvili); Department of Molecular Cell Biology, Weizmann Institute of Science, Rehovot, Israel (Mayo); Sagol School of Neuroscience, Tel Aviv University, Tel Aviv, Israel (Efrati).

Corresponding Author: Keren Doenyas-Barak, MD, Sagol Center for Hyperbaric Treatment and Research, Shamir Medical Center, Einat 1, Zerifin 70300, Israel (kerendoenyas@gmail.com).

Relevant Financial Relationships: Dr Efrati is a shareholder at AVIV Scientific LTD. **Dr Hadanny** works for AVIV Scientific LTD. The remaining authors have no competing interests.

Funding/Support: None.

Supplementary Material: Available at Psychiatrist.com.

References

1. American Psychiatric Association. *Diagnostic and Statistical Manual of Mental Disorders*. 5th ed. American Psychiatric Publishing; 2013:591–643.
2. Levi O, Ben Yehuda A, Pine DS, et al. A sobering look at treatment effectiveness of military-related posttraumatic stress disorder. *Clin Psychol Sci*. 2022;10(4):690–699.
3. Forbes D, Creamer M, Bisson JI, et al. A guide to guidelines for the treatment of PTSD and related conditions. *J Trauma Stress*. 2010;23(5):537–552.
4. Phelps AJ, Steele Z, Cowlishaw S, et al. Treatment outcomes for military veterans with posttraumatic stress disorder: response trajectories by symptom cluster. *J Trauma Stress*. 2018;31(3):401–409.
5. Maguen S, Madden E, Holder N, et al. Effectiveness and comparative effectiveness of evidence-based psychotherapies for posttraumatic stress disorder in clinical practice. *Psychol Med*. 2023;53(2):419–428.
6. Gold AL, Shin LM, Orr SP, et al. Decreased regional cerebral blood flow in medial prefrontal cortex during trauma-unrelated stressful imagery in Vietnam veterans with post-traumatic stress disorder. *Psychol Med*. 2011;41(12):2563–2572.
7. Pitman RK, Rasmusson AM, Koenen KC, et al. Biological studies of post-traumatic stress disorder. *Nat Rev Neurosci*. 2012;13(11):769–787.
8. Sartory G, Cwik J, Knuppertz H, et al. In search of the trauma memory: a meta-analysis of functional neuroimaging studies of symptom provocation in posttraumatic stress disorder (PTSD). *PLoS One*. 2013;8(3):e58150.
9. van Rooij SJH, Kennis M, Vink M, et al. Predicting treatment outcome in PTSD: a longitudinal functional MRI study on trauma-unrelated emotional processing. *Neuropsychopharmacology*. 2016;41(4):1156–1165.
10. Liu Z, Xiao X, Zhang K, et al. Dynamic brain network changes in resting-state reflect neuroplasticity: molecular and cognitive evidence. *BioRxiv*. 2019:695122.
11. Hadanny A, Efrati S. The hyperoxic-hypoxic paradox. *Biomolecules*. 2020;10(6):958.
12. Hadanny A, Bechor Y, Catalogna M, et al. Hyperbaric oxygen therapy can induce neuroplasticity and significant clinical improvement in patients suffering from fibromyalgia with a history of childhood sexual abuse-randomized controlled trial. *Front Psychol*. 2018;9:2495.
13. Efrati S, Fishlev G, Bechor Y, et al. Hyperbaric oxygen induces late neuroplasticity in post stroke patients—randomized, prospective trial. *PLoS One*. 2013;8(1):e53716.
14. Ablin JN, Lang E, Catalogna M, et al. Hyperbaric oxygen therapy compared to pharmacological intervention in fibromyalgia patients following traumatic brain injury: a randomized, controlled trial. *PLoS One*. 2023;18(3):e0282406.
15. Tal S, Hadanny A, Berkovitz N, et al. Hyperbaric oxygen may induce angiogenesis in patients suffering from prolonged post-concussion syndrome due to traumatic brain injury. *Restor Neurol Neurosci*. 2015;33(6):943–951.
16. Boussi-Gross R, Golan H, Fishlev G, et al. Hyperbaric oxygen therapy can improve post concussion syndrome years after mild traumatic brain injury - randomized prospective trial. *PLoS One*. 2013;8(11):e79995.
17. Zilberman-Itskovich S, Catalogna M, Sasson E, et al. Hyperbaric oxygen therapy improves neurocognitive functions and symptoms of post-COVID condition: randomized controlled trial. *Sci Rep*. 2022;12(1):11252.
18. Doenyas-Barak K, Catalogna M, Kutz I, et al. Hyperbaric oxygen therapy improves symptoms, brain's microstructure and functionality in veterans with treatment resistant post-traumatic stress disorder: a prospective, randomized, controlled trial. *PLoS One*. 2022;17(2):e0264161.

19. Doenyas-Barak K, Kutz I, Levi G, et al. Hyperbaric oxygen therapy for veterans with treatment-resistant PTSD: a longitudinal follow-up study. *Mil Med*. 2023; 188(7–8):e2227–e2233.
20. Harch PG, Andrews SR, Rowe CJ, et al. Hyperbaric oxygen therapy for mild traumatic brain injury persistent postconcussion syndrome: a randomized controlled trial. *Med Gas Res*. 2020;10(1):8–20.
21. Mozayeni BR, Duncan W, Zant E, et al. The National Brain Injury, Rescue and Rehabilitation Study–a multicenter observational study of hyperbaric oxygen for mild traumatic brain injury with post-concussive symptoms. *Med Gas Res*. 2019; 9(1):1–12.
22. Weaver LK, Wilson SH, Lindblad AS, et al. Hyperbaric oxygen for post-concussive symptoms in United States military service members: a randomized clinical trial. *Undersea Hyperb Med*. 2018;45(2):129–156.
23. Harch PG, Andrews SR, Fogarty EF, et al. A phase I study of low-pressure hyperbaric oxygen therapy for blast-induced post-concussion syndrome and post-traumatic stress disorder. *J Neurotrauma*. 2012;29(1):168–185.
24. Harch PG, Andrews SR, Fogarty EF, et al. Case control study: hyperbaric oxygen treatment of mild traumatic brain injury persistent post-concussion syndrome and post-traumatic stress disorder. *Med Gas Res*. 2017;7(3):156–174.
25. Cifu DX, Hart BB, West SL, et al. The effect of hyperbaric oxygen on persistent postconcussion symptoms. *J Head Trauma Rehabil*. 2014;29(1):11–20.
26. Miller RS, Weaver LK, Bahraini N, et al. Effects of hyperbaric oxygen on symptoms and quality of life among service members with persistent postconcussion symptoms: a randomized clinical trial. *JAMA Intern Med*. 2015;175(1):43–52.
27. Wolf G, Cifu D, Baugh L, et al. The effect of hyperbaric oxygen on symptoms after mild traumatic brain injury. *J Neurotrauma*. 2012;29(17):2606–2612.
28. Hadanny A, Hachmo Y, Rozali D, et al. Effects of hyperbaric oxygen therapy on mitochondrial respiration and physical performance in middle-aged athletes: a blinded, randomized controlled trial. *Sports Med Open*. 2022;8(1):22.
29. Varker T, Kartal D, Watson L, et al. Defining response and nonresponse to posttraumatic stress disorder treatments: a systematic review. *Clin Psychol Sci Pract*. 2020;27(4):e12355.
30. Weathers FW, Bovin MJ, Lee DJ, et al. The Clinician-Administered PTSD Scale for DSM–5 (CAPS-5): development and initial psychometric evaluation in military veterans. *Psychol Assess*. 2018;30(3):383–395.
31. Beck AT, Steer RA, Brown GK. Beck depression inventory. *Springer*. 1996.
32. Antony MM, Bieling PJ, Cox BJ, et al. Psychometric properties of the 42-item and 21-item versions of the Depression Anxiety Stress Scales in clinical groups and a community sample. *Psychol Assess*. 1998;10(2):176–181.
33. Martenyi F, Brown EB, Zhang H, et al. Fluoxetine versus placebo in posttraumatic stress disorder. *J Clin Psychiatry*. 2002;63(3):199–206.
34. Yoshii T. The role of the thalamus in post-traumatic stress disorder. *Int J Mol Sci*. 2021;22(4):1730.
35. Doenyas-Barak K, Kutz I, Lang E, et al. Memory surfacing among veterans with PTSD receiving hyperbaric oxygen therapy. *Undersea Hyperb Med*. 2023;50(4): 395–401.
36. Abinader EG, Sharif D, Rauchfleich S, et al. Effect of low altitude (Dead Sea location) on exercise performance and wall motion in patients with coronary artery disease. *Am J Cardiol*. 1999;83(2):250–251, A5.
37. MacLaughlin KJ, Barton GP, Braun RK, et al. Hyperbaric air mobilizes stem cells in humans; a new perspective on the hormetic dose curve. *Front Neurol*. 2023;14: 1192793.
38. Hadanny A, Hachmo Y, Rozali D, et al. Effects of hyperbaric oxygen therapy on mitochondrial respiration and physical performance in middle-aged athletes: a blinded, randomized controlled trial. *Sports Med Open*. 2022;8(1):22.
39. Weaver LK, Churchill SK, Bell J, et al. A blinded trial to investigate whether "pressure-familiar" individuals can determine chamber pressure. *Undersea Hyperb Med*. 2012;39(4):801–805.
40. Churchill S, Deru K, Weaver LK, et al. Adverse events and blinding in two randomized trials of hyperbaric oxygen for persistent post-concussive symptoms. *Undersea Hyperb Med*. 2019;46(3):331–340.
41. Weaver LK, Deru K, Churchill S, et al. A randomized trial of one versus three hyperbaric oxygen sessions for acute carbon monoxide poisoning. *Undersea Hyperb Med*. 2023;50(3):325–342.
42. Stelson EA, Bolenbaugh M, Woods-Jaeger B, et al. Identifying research Participation effects through qualitative methods: feedback from Research Engagement Consultants involved in a pediatric mental health comparative effectiveness trial. *SSM-Qualitative Res Health*. 2021;1:100023.
43. Etkin A, Wager TD. Functional neuroimaging of anxiety: a meta-analysis of emotional processing in PTSD, social anxiety disorder, and specific phobia. *Am J Psychiatry*. 2007;164(10):1476–1488.
44. Olson EA, Kaiser RH, Pizzagalli DA, et al. Regional prefrontal resting-state functional connectivity in posttraumatic stress disorder. *Biol Psychiatry Cogn Neurosci Neuroimaging*. 2019;4(4):390–398.
45. Shaw SB, Terpou BA, Densmore M, et al. Large-scale functional hyperconnectivity patterns in trauma-related dissociation: an rs-fMRI study of PTSD and its dissociative subtype. *Nat Ment Health*. 2023;1(10):711–721.
46. Peterson K, Bourne D, Anderson J, et al. *Evidence Brief: Hyperbaric Oxygen Therapy (HBOT) for Traumatic Brain Injury and/or Post-Traumatic Stress Disorder*. Department of Veterans Affairs (US); 2018.
47. Doenyas-Barak K, Kutz I, Lang E, et al. The use of hyperbaric oxygen for veterans with PTSD: basic physiology and current available clinical data. *Front Neurosci*. 2023;17:1259473.

The Journal of Clinical Psychiatry

Supplementary Material

Article Title: Hyperbaric Oxygen Therapy for Veterans Suffering from Combat-Associated Posttraumatic Stress Disorder: A Randomized, Sham-Controlled Clinical Trial

Authors: Keren Doenyas-Barak, MD; Ilan Kutz, MD; Erez Lang, MD; Amir Assouline, PhD; Amir Hadanny, MD, PhD; Kristoffer C. Aberg, PhD; Gabriela Levi; Ilia Beberashvili, MD; Avi Mayo, PhD; and Shai Efrati, MD

DOI Number: 10.4088/JCP.24m15464

LIST OF SUPPLEMENTARY MATERIAL FOR THE ARTICLE

DISCLAIMER

BOLD Preprocessing

Functional and anatomical data were preprocessed using a flexible preprocessing pipeline[4] including realignment with correction of susceptibility distortion interactions, slice timing correction, outlier detection, direct segmentation and MNI-space normalization and smoothing. Functional data were realigned using SPM realign & unwarp procedure[5], where all scans were coregistered to a reference image using the least squares approach and a 6 parameter (rigid body) transformation[6], and resampled using b-spline interpolation to correct for motion and magnetic susceptibility interactions.

Temporal misalignment between different slices of the functional data (acquired in ascending order) was corrected following SPM slice-timing correction (STC) procedure[7,8], using sinc temporal interpolation to resample each BOLD slice timeseries to a common mid-acquisition time. Potential outlier slices were identified using ART[9] as acquisitions with framewise displacement above 0.9 mm or global BOLD signal changes above 5 standard deviations[10,11], and a reference BOLD image was computed for each subject by averaging the slices excluding outliers.

Functional and anatomical data were normalized into standard MNI space, segmented into grey matter, white matter, and cerebrospinal fluid (CSF) tissue classes, and resampled to 2 mm isotropic voxels following a direct normalization procedure[11,12] using SPM unified segmentation and normalization algorithm[13,14] with the default IXI-549 tissue probability map template.

Functional data were smoothed using spatial convolution with a Gaussian kernel of 8 mm full width half maximum (FWHM).

Functional data were then denoised using a standard denoising pipeline[15] including the regression of potential confounding effects characterized by white matter timeseries (5 CompCor noise components), CSF timeseries (5 CompCor noise components), outlier scans (below 85 factors)[10], motion parameters and their first order derivatives (12 factors)[16], session and task effects and their first order derivatives (4 factors), and linear trends (2 factors) within each functional run, followed by bandpass frequency filtering of the BOLD timeseries[17] between 0.008 Hz and 0.09 Hz. CompCor[18,19] noise components within white matter and CSF were estimated by computing the average BOLD signal as well as the largest principal components orthogonal to the BOLD average, motion parameters, and outlier scans within each subject's eroded segmentation masks. From the number of noise terms included in this denoising strategy, the effective degrees of

freedom of the BOLD signal after denoising were estimated to range from 101.6 to 133.8 (average 131.1) across all subjects[11].

BOLD analysis

First-level analysis (individual maps)

Seed-based connectivity maps (SBC) and region of interest (ROI)-to-ROI connectivity matrices (RRC) were estimated characterizing the patterns of functional connectivity with 23 HPC-ICA networks[2] and Harvard-Oxford atlas ROIs[20]. The ROIs examined included PTSD commonly reported large-scale brain networks: default mode (DMN), salience (SN), fronto-parietal (FPN), thalami, amygdala and hippocampi . Functional connectivity strength was represented by Fisher-transformed bivariate correlation coefficient from a weighted general linear model (weighted-GLM[21]), defined separately for each pair of seed and target area. Individual scans were weighted by a boxcar signal characterizing each individual task or experimental condition convolved with an SPM canonical hemodynamic response function and rectified.

Second-level analysis (group-level analyses)

Second-level were performed using a General Linear Model (GLM)[22]. For each individual voxel a separate GLM was estimated, with first-level connectivity measures at this voxel as dependent variables (one independent sample per subject and one measurement per task or experimental condition, if applicable), and groups or other subject-level identifiers as independent variables. Voxel-level hypotheses were evaluated using multivariate parametric statistics with random-effects across subjects and sample covariance estimation across multiple measurements.

Inferences were performed at the level of individual clusters (groups of contiguous voxels). Cluster-level inferences were based on parametric statistics from Gaussian Random Field theory[23,24].

Results were thresholded using a combination of a cluster-forming $p < 0.001$-0.005 voxel-level threshold, and a familywise corrected p-FDR < 0.05 cluster-size threshold[25].

References

[1] Whitfield-Gabrieli, S., & Nieto-Castanon, A. (2012). Conn: a functional connectivity toolbox for correlated and anticorrelated brain networks. Brain connectivity, 2(3), 125-141.

[2] Nieto-Castanon, A. & Whitfield-Gabrieli, S. (2017). CONN functional connectivity toolbox: RRID SCR_009550, release 17. doi:10.56441/hilbertpress.1744.6736.

[3] Penny, W. D., Friston, K. J., Ashburner, J. T., Kiebel, S. J., & Nichols, T. E. (Eds.). (2011). Statistical parametric mapping: the analysis of functional brain images. Elsevier.

[4] Nieto-Castanon, A. (2020). FMRI minimal preprocessing pipeline. In Handbook of functional connectivity Magnetic Resonance Imaging methods in CONN (pp. 3–16). Hilbert Press.

[5] Andersson, J. L., Hutton, C., Ashburner, J., Turner, R., & Friston, K. J. (2001). Modeling geometric deformations in EPI time series. Neuroimage, 13(5), 903-919.

[6] Friston, K. J., Ashburner, J., Frith, C. D., Poline, J. B., Heather, J. D., & Frackowiak, R. S. (1995). Spatial registration and normalization of images. Human brain mapping, 3(3), 165-189.

[7] Henson, R. N. A., Buechel, C., Josephs, O., & Friston, K. J. (1999). The slice-timing problem in event-related fMRI. NeuroImage, 9, 125.

[8] Sladky, R., Friston, K. J., Tröstl, J., Cunnington, R., Moser, E., & Windischberger, C. (2011). Slice-timing effects and their correction in funct ional MRI. Neuroimage, 58(2), 588-594.

[9] Whitfield-Gabrieli, S., Nieto-Castanon, A., & Ghosh, S. (2011). Artifact detection tools (ART). Cambridge, MA. Release Version, 7(19), 11.

[10] Power, J. D., Mitra, A., Laumann, T. O., Snyder, A. Z., Schlaggar, B. L., & Petersen, S. E. (2014). Methods to detect, characterize, and remove motion artifact in resting state fMRI. Neuroimage, 84, 320-341.

[11] Nieto-Castanon, A. (submitted). Preparing fMRI Data for Statistical Analysis. In M. Filippi (Ed.). fMRI techniques and protocols. Springer. doi:10.48550/arXiv.2210.13564

[12] Calhoun, V.D., Wager, T.D., Krishnan, A., Rosch, K.S., Seymour, K.E., Nebel, M.B., Mostofsky, S.H., Nyalakanai, P. and Kiehl, K. (2017). The impact of T1 versus EPI spatial normalization templates for fMRI data analyses (Vol. 38, No. 11, pp. 5331-5342).

[13] Ashburner, J., & Friston, K. J. (2005). Unified segmentation. Neuroimage, 26(3), 839-851.

[14] Ashburner, J. (2007). A fast diffeomorphic image registration algorithm. Neuroimage, 38(1), 95-113.

[15] Nieto-Castanon, A. (2020). FMRI denoising pipeline. In Handbook of functional connectivity Magnetic Resonance Imaging methods in CONN (pp. 17–25). Hilbert Press.

[16] Friston, K. J., Williams, S., Howard, R., Frackowiak, R. S., & Turner, R. (1996). Movement-related effects in fMRI time-series. Magnetic resonance in medicine, 35(3), 346-355.

[17] Hallquist, M. N., Hwang, K., & Luna, B. (2013). The nuisance of nuisance regression: spectral misspecification in a common approach to resting-state fMRI preprocessing reintroduces noise and obscures functional connectivity. Neuroimage, 82, 208-225.

[18] Behzadi, Y., Restom, K., Liau, J., & Liu, T. T. (2007). A component based noise correction method (CompCor) for BOLD and perfusion based fMRI. Neuroimage, 37(1), 90-101.

[19] Chai, X. J., Nieto-Castanon, A., Ongur, D., & Whitfield-Gabrieli, S. (2012). Anticorrelations in resting state networks without global signal regression. Neuroimage, 59(2), 1420-1428.

[20] Desikan R.S., Ségonne F., Fischl B., Quinn B.T., Dickerson B.C., Blacker D., Buckner R.L., Dale A.M., Maguire R.P., Hyman B.T., Albert M.S., & Killiany R.J. (2006) An automated labeling system for subdividing the human cerebral cortex on MRI scans into gyral based regions of interest. Neuroimage 31(3):968-980

[21] Nieto-Castanon, A. (2020). Functional Connectivity measures. In Handbook of functional connectivity Magnetic Resonance Imaging methods in CONN (pp. 26–62). Hilbert Press.

[22] Nieto-Castanon, A. (2020). General Linear Model. In Handbook of functional connectivity Magnetic Resonance Imaging methods in CONN (pp. 63–82). Hilbert Press.

[23] Worsley, K. J., Marrett, S., Neelin, P., Vandal, A. C., Friston, K. J., & Evans, A. C. (1996). A unified statistical approach for determining significant signals in images of cerebral activation. Human brain mapping, 4(1), 58-73.

[24] Nieto-Castanon, A. (2020). Cluster-level inferences. In Handbook of functional connectivity Magnetic Resonance Imaging methods in CONN (pp. 83–104). Hilbert Press.

[25] Chumbley, J., Worsley, K., Flandin, G., & Friston, K. (2010). Topological FDR for neuroimaging. Neuroimage, 49(4), 3057-3064.

Supplementary Figure 1: Confusion Matrix

Confusion matrix showing treatment perception in the two groups. Accuracy was calculated as the true perceived HBOT or sham divided by the total participants. Recall was calculated as the number of true HBOT perceptions divided by the total actual HBOT perceptions. Precision was calculated as the number of true HBOT perceptions divided by the sum of true HBOT perceptions and false sham perceptions.

		Predicted condition	
		HBOT 36	SHAM 20
Actual condition	HBOT 28	True HBOT 18	False SHAM 10
	SHAM 28	False HBOT 18	True SHAM 10

Accuracy	0.5
Recall	0.642857
Precision	0.5

Supplementary Table 1:

Significant seed to voxel functional connectivity group-by-time interactions

Seed	**Regions**	**MNI coordinate**	**Cluster-size (voxels)**

Thalamus - Left	Right inferior parietal lobe-Supramarginal Gyrus(r) Angular gyrus(r) Supramarginal Gyrus(l)	54,-40,50 48,-52,50 -56,-36,44	242 227 204
Thalamus -Right	Middle Frontal Gyrus (l)	-38,26,38	351
DMN -mPFC (1,55,-3)	Lingual Gyrus(r) Intracalcarine Cortex (l)	8,-82,-8 -10,-84,6	208 125
FPN DLPFC -left (-43,38,28)	Thalamus (r) Thalamus (l)	10,-8,8 -14,-16,10	175 94
FPN DLPFC -right (41,38,30)	Supramarginal gyrus(r) Supramarginal gyrus(l) Angular gyrus(r) Angular gyrus(l) Putamen(r) Putamen(l) Insular cortex Precuneus Frontal pole(r)	52 -40 40 -56 -48 42 56 -50 38 -48 -54 48 28 0 4 -26 -4 4 36 -4 8 6 -66 50 34 46 18	412 222 141 127 326 299 176 220 350
Salience RPFC - left (-32,45,27)	Frontal Pole(r)	40,52,4	765

Salience **RPFC-** right (32,45, 27)	Frontal Pole(r) Superior frontal gyrus (r)	38,54,12 18,14,64	228 179